THE JOURNAL OF BIOLOGICAL CHEMISTRY
Vol. 278, No. 49, Issue of December 5, pp. 48914–48920, 2003

Printed in U.S.A.

A Self-sufficient Cytochrome P450 with a Primary Structural Organization That Includes a Flavin Domain and a [2Fe-2S] Redox Center*

Received for publication, August 29, 2003, and in revised form, September 22, 2003
Published, JBC Papers in Press, September 27, 2003, DOI 10.1074/jbc.M309630200

Gareth A. Roberts, Ayhan Çelik, Dominic J. B. Hunter, Tobias W. B. Ost, John H. White, Stephen K. Chapman, Nicholas J. Turner, and Sabine L. Flitsch‡

From the Edinburgh Centre for Protein Technology, School of Chemistry, University of Edinburgh, The King's Buildings, West Mains Road, Edinburgh EH9 3JJ, United Kingdom

P450 RhF from *Rhodococcus* sp. NCIMB 9784 is the first example of a new class of cytochrome P450 in which electrons are supplied by a novel, FMN- and Fe/S-containing, reductase partner in a fused arrangement. We have previously cloned the gene encoding the enzyme and shown it to comprise an N-terminal P450 domain fused to a reductase domain that displays similarity to the phthalate family of oxygenase reductase proteins. A reductase of this type had never previously been reported to interact with a cytochrome P450. In this report we describe the purification and partial characterization of P450 RhF. We show that the enzyme is self-sufficient in catalyzing the *O*-dealkylation of 7-ethoxycoumarin. The P450 RhF catalyzed *O*-dealkylation of 7-ethoxycoumarin is inhibited by several compounds that are known inhibitors of cytochrome P450. Pre-steady state kinetic analysis indicates that P450 RhF shows a 500-fold preference for NAPDH over NADH in terms of K_d value (6.6 μM *versus* 3.7 mM, respectively). Potentiometric studies show reduction potentials of −243 mV for the two-electron reduction of the FMN and −423 mV for the heme (in the absence of substrate).

Cytochrome P450 is a superfamily of monooxygenase enzymes with diverse catalytic activities. These have been found in all three phylogenetic domains of life, including many higher animal tissues. The primary chemical reaction catalyzed by these monooxygenases is the two-electron activation of molecular dioxygen, whereby one oxygen atom is inserted into the substrate with concomitant reduction of the second atom to water. NAD(P)H provides the required electron equivalents via a number of different redox partners (1).

Depending on the nature of the redox partner, P450 enzymes generally fall into two broad classes. Class I enzymes are three-component systems comprising an NAD(P)H-binding flavoprotein reductase, a small iron-sulfur protein, and the P450. These enzymes are found in the mitochondrial membranes of eukaryotes and in most bacteria. Class II enzymes are two-component systems comprising an FAD- and FMN-containing NADPH reductase (in which FAD and FMN are in an equimolar ratio) and the P450. This type of P450 is found almost exclusively in eukaryotes in association with the endoplasmic reticulum, where they play a major role in the oxidative metabolism of a wide spectrum of substrates including xenobiotics, endogenous fatty acids, steroids, leukotrienes, prostaglandins, and vitamins.

There are, however, examples of cytochrome P450 that cannot readily be defined as a member of either of these two classes. P450 BM3 (CYP102A1) from *Bacillus megaterium*, which oxidizes long chain fatty acids, comprises a diflavin reductase fused to the P450 to form a catalytically self-sufficient single polypeptide enzyme (2, 3). P450 BM3 has been likened to a fused eukaryotic class II enzyme. However, since its primary structural organization is quite distinct from the class II enzymes, P450 BM3 is regarded as the first example of a new, self-sufficient, class of P450 enzyme. Two further examples of P450 enzymes of this type (CYP102A2 and CYP102A3) from *Bacillus subtilis* were identified as a result of a whole genome sequencing project (4). A BM3-like P450 from the actinomycete *Actinosynnema pretiosum*, which is thought to be involved in the biosynthesis of the polyketide antitumor agent ansamitocin, has also been described (5). Two membrane-bound eukaryotic counterparts of P450 BM3 have been cloned from *Fusarium oxysporum* (6) and *Fusarium verticillioides* (7). Recently, a search against a data base of unfinished genome sequencing projects identified three more examples from *Bacillus anthracis* (Ames strain), *Bacillus cereus*, and the β-proteobacterium *Ralstonia metallidurans* (8).

During a PCR-based screen for new P450 activities from actinomycetes, we cloned a novel P450 gene from *Rhodococcus* sp. NCIMB 9784 (previously classified as *Corynebacterium* sp. Strain T1), which was of unique primary structural organization (9). Surprisingly, an analysis of the gene revealed that it encoded a heme domain fused to a reductase displaying convincing similarity to the phthalate family of dioxygenase reductases. We named the enzyme P450 RhF to reflect both its origin and the fused nature of the gene product. Despite the fact that proteins homologous to the C-terminal reductase portion of P450 RhF have been found in a diverse range of organisms, this was the first time an oxidoreductase of this type had been implicated in partnering a P450 enzyme. The N-terminal heme portion of the enzyme displays striking similarity to the thiocarbamate-inducible P450 from *Rhodococcus erythropolis* NI86/21 (ThcB), a class I enzyme of the CYP116 family (10). Working independently, De Mot and Parret (8) identified four putative homologues to P450 RhF from three pathogenic *Burkholderia* species and the heavy metal-resistant bacterium *R. metallidurans* by analyzing unfinished genomes with the ThcB sequence.

* This work was supported in part by the Biotechnology and Biological Research Council (BBSRC) and Department of Trade and Industry (DTI) under the aegis of a LINK program and GlaxoSmithKline (GSK), Pfizer, Ultrafine Chemicals, and the Edinburgh Protein Interaction Centre (Wellcome Trust). The costs of publication of this article were defrayed in part by the payment of page charges. This article must therefore be hereby marked "*advertisement*" in accordance with 18 U.S.C. Section 1734 solely to indicate this fact.

‡ To whom correspondence should be addressed. Tel.: 44-131-650-4737; Fax: 44-131-650-4743; E-mail: s.flitsch@ed.ac.uk.

We have previously shown that a recombinant strain of *Escherichia coli* expressing the gene for P450 RhF was able to dealkylate 7-ethoxycoumarin, whereas the same strain lacking this gene was unable to do so. However, in these whole cell studies we could not definitively demonstrate that the enzyme was catalytically self-sufficient due to the possible involvement of endogenous electron transfer proteins. In this report we describe the isolation and partial characterization of recombinant P450 RhF.

EXPERIMENTAL PROCEDURES

Enzymes and Chemicals—All chemicals were purchased from Sigma-Aldrich. Biotinylated thrombin was supplied by Novagen (Madison, WI). A protease inhibitor mixture containing 4-(2-aminoethyl)benzenesulfonyl fluoride, bestatin, pepstatin A, *trans*-epoxysuccinyl-L-leucylamido(4-guanido)butane, and *N*-(α-rhamnopyranosyloxyhydroxyphosphinyl)-Leu-Trp-(phosphoramidon) was supplied by Sigma-Aldrich. Restriction endonucleases, T4 DNA ligase, *Vent* DNA polymerase, and calf intestinal alkaline phosphatase were from New England Biolabs (Beverly, MA).

Maintenance and Growth of Microorganisms—Rhodococcus sp. NCIMB 9784 was obtained from the National Culture of Industrial and Marine Bacteria (Aberdeen, UK). The strain was maintained on nutrient agar slopes at room temperature, and grown in Luria-Bertani (LB) medium (11) at 30 °C in baffled flasks. *E. coli* XL2-Blue MRF' ultracompetent cells were purchased from Stratagene (La Jolla, CA) and grown in LB medium at 37 °C. *E. coli* BL21(DE3) cells were obtained from Invitrogen (Groningen, The Netherlands) and grown at 30 °C in LB medium unless stated otherwise. Ampicillin was used at 100 μg/ml when required for selection of plasmid on both liquid and solid medium. pET14b used in the expression studies was obtained from Novagen.

DNA Manipulations—Standard DNA procedures were used throughout (11). Total DNA was prepared from *Rhodococcus* sp. NCIMB 9784 as described previously (12). The full-length gene encoding P450 RhF was cloned into pET14b for expression to give a fusion protein with a 20-residue N-terminal prepeptide, which includes a His_6 tag and a thrombin cleavage site. The P450 RhF gene was amplified by PCR and cloned into the expression vector. The forward and reverse primers for the amplification were 5′-CGGTGTCCATATGAGTGCATCAGTTCCGGCG-3′ and 5′-AGGTTGATCATTCAGAGTCGCAGGGCCAGCC-3′, respectively. The NdeI and BclI restriction endonuclease sites used for the subsequent cloning of the PCR product are underlined.

The PCR consisted of 30 cycles, with denaturation at 94 °C for 1 min 30 s, annealing at 60 °C for 45 s and extension for 2 min 30 s at 72 °C. The initial denaturation step was at 95 °C for 2 min. The PCR mix included *Vent* DNA polymerase (New England Biolabs, MS), 10 mM Tris-HCl (pH 9.0 at room temperature), 50 mM KCl, 1.5 mM $MgCl_2$, 200 μM of each deoxynucleoside triphosphate, 40 pM of each primer, 10% (v/v) dimethyl sulfoxide, and ~50 ng of *Rhodococcus* sp. NCIMB 9784 total genomic DNA as template in a reaction volume of 50 μl.

The PCR product was isolated and digested with NdeI and BclI restriction endonucleases. The digested DNA was purified and cloned into the NdeI and BamHI sites of the pET14b vector to give the final expression construct (pAG04). Plasmid construction was performed in *E. coli* XL1-Blue MRF′. The insert DNA was sequenced to ensure no mistakes had been introduced during the amplification process. pAG04 was then transformed into the expression strain *E. coli* BL21(DE3).

Production of His_6-P450 RhF—E. coli BL21(DE3) containing the expression construct was grown in LB medium containing 100 μg/ml ampicillin at 30 °C. We had previously demonstrated that a non-tagged version of P450 RhF was synthesized in a largely insoluble form when the culture temperature was elevated to 37 °C (9). After induction with 1 mM *IPTG*[1] at an optical density (OD_{600}) of 0.8, growth was continued for up to 4 h before harvesting. Aliquots were withdrawn at regular time points. Expression was assessed by comparing the banding pattern obtained by SDS-PAGE analysis of whole cell extracts with that of a negative control (*i.e. E. coli* BL21(DE3)pET14b). The solubility of the protein was assessed by a standard procedure (11).

Although expression was found to be constitutive, we followed the standard induction protocol using IPTG for protein purification studies. Typically a starter culture (100 ml of LB containing 100 μg/ml ampicillin) was grown to an optical density of ~0.8–1.0 from a single colony (~16 h growth at 30 °C) using a baffled shake flask. This was then used to inoculate 10 liters of LB medium (containing 100 μg/ml ampicillin) in a fermentor (Bioflo 4500, New Brunswick Scientific, Edison, NJ). When the OD_{600} reached 0.4 (after ~4 h growth) expression of the recombinant gene was induced by adding 1 mM IPTG. Cells were harvested 3 h after IPTG induction and stored at −20 °C. Typically, using this protocol, we obtained about 20–25 g of cell paste from 10 liters of broth.

Protein Purification—Approximately 20 g of cell paste was suspended in 20 ml of ice-cold buffer A (25 mM Tris-HCl, pH 7.8, 300 mM NaCl, 10% (v/v) glycerol) containing 0.1 mM phenylmethylsulfonyl fluoride, and 200 μl of protease inhibitor mixture (Sigma-Aldrich). The cells were disrupted by sonication using a Soniprep 150 sonicator (Sanyo, Tokyo, Japan) fitted with a 9-mm diameter probe. The cell suspension was split into two equal volumes for disruption and each aliquot was kept on ice and sonicated with a 15 s burst followed by a 45 s interval. This process was repeated 12 times. The resulting cell extract was centrifuged at 48,000 × *g* for 20 min at 4 °C. The cell-free extract was carefully removed and filtered through a 0.45-micron filter unit. The clarified extract was then loaded onto a 5-ml Nickel HiTrap column (Amersham Biosciences), equilibrated in buffer A at a flow rate of 1 ml/min. Column chromatography was performed at 4 °C. The column was then extensively washed with buffer A (12 column volumes) to remove unbound material. The majority of contaminating proteins were then removed by washing with 30 mM imidazole in buffer A (10 column volumes) before elution of the recombinant His-tagged P450RhF by 300 mM imidazole in buffer A.

The buffer was exchanged using a PD-10 desalting column (Amersham Biosciences) which was equilibrated in Buffer B (50 mM Tris-HCl, pH 7.8, 10% (v/v) glycerol, 0.5 mM dithiothreitol) at 4 °C. The small amount of contaminating protein was removed by anion exchange chromatography. The protein sample (~7.0 ml) was loaded onto a Resource-Q column (6 ml) (Amersham Biosciences) at a flow rate of 3 ml/min. The column was then washed with two column volumes of Buffer B. Protein was eluted using a linear gradient of 0–1.0 M NaCl in buffer B over 20 column volumes. P450 RhF was eluted in ~250 mM NaCl.

The sample volume (~4 ml) was reduced to 1 ml using a spin concentrator with a 30 kDa cut-off membrane (Sartorius, Goettingen, Germany). Glycerol was added to a final concentration of 50% (v/v) and the sample stored at −20 °C.

Removal of the N-terminal His Tag—The N-terminal His tag was removed using biotinylated thrombin. Typically, 1.0 unit of thrombin was incubated with 200 μg of P450 RhF at 22 °C for 90 min. Biotinylated thrombin was subsequently removed using streptavidin agarose. Protein was then recovered by spin-filtration. The extent of cleavage was determined by both Western blot analysis using an anti-His tag antibody and by mass spectrometry.

Mass Spectrometry—Mass spectrometry of the intact recombinant P450 RhF was performed by MALDI-TOF using a Voyager DE STR instrument (Applied Biosystems, Foster City, CA). Protein samples were diluted in 0.1% trifluoroacetic acid to ~0.05 mg/ml and mixed with an equal volume of matrix (saturated solution of sinapinic acid in 50% acetonitrile, 0.1% trifluoroacteic acid) on a stainless steel surface. The samples were air dried at room temperature to crystallize. The machine was operated in positive ion mode and calibrated with conalbumin and bovine serum albumin.

Western Blotting—Protein samples were resolved on 10–20% SDS-PAGE gels and electroblotted onto a nitrocellulose membrane (Hybond ECL, Amersham Biosciences) using a Bio-Rad transblot cell at a constant current of 150 mA for 90 min. After blocking in 5% (w/v) dried milk powder the blot was subjected to immunodetection using mouse monoclonal anti-polyhistidine antibody peroxidase conjugate (Sigma-Aldrich) diluted 1:1000. Following extensive washing the blot was developed using 3,3′-diaminobenzidine in urea/hydrogen peroxide (FAST DAB tablets, Sigma-Aldrich) according to the manufacturers' guidelines.

Spectroscopic Analysis—The homogeneity of the protein preparation was assessed by SDS-PAGE using a 10–20% gradient gel. The spectral properties (ratio of P450-specific absorption at 420 nm compared with protein-specific absorption at 280 nm) were also measured. The cytochrome P450 concentration was determined by the method described in the literature (13), using an extinction coefficient of $\epsilon_{450-490} = 91\ mM^{-1}\ cm^{-1}$.

Absorption spectra of P450 RhF in the UV-visible region were recorded with a Shimadzu UV-2101PC scanning spectrophotometer (Shimadzu, Duisburg, Germany) using a 1-cm pathlength quartz cell. Spectra were recorded using ~0.1–0.2 μM P450 RhF in phosphate buffer (50 mM potassium phosphate buffer, pH 7.8, 10% (v/v) glycerol). Spectra of the reduced enzyme were recorded after the addition of a few grains of

[1] The abbreviations used are: IPTG, isopropyl-β-D-thiogalactopyranoside; MALDI-TOF, matrix-assisted laser desorption ionization time-of-flight; OTTLE, optically transparent thin layer electrochemical.

sodium dithionite. Reduced enzyme was reacted with CO by gently bubbling CO gas into a solution of reduced P450 RhF.

Presteady State Kinetics—Presteady state measurements on the reduction of P450 RhF by either NADPH or NADH were performed at 25 °C using an Applied Photophysics stopped-flow spectrophotometer (SX.17MV) contained within an anaerobic glove box (Belle Technology, Portesham, UK; $[O_2] < 5$ ppm) using either single-wavelength or diode-array detectors. Enzyme and nucleotide solutions were made up in 50 mM Tris-HCl, pH 7.5, 100 mM NaCl, 10% (v/v) glycerol. Concentrations were checked spectrophotometrically before use. FMN reductions were recorded at 462 nm, and the resultant traces analyzed using Origin 7 software (Microcal, Northampton, MA).

Steady State Kinetics—The P450 RhF catalyzed formation of 7-hydroxycoumarin from 7-ethoxycoumarin was monitored directly by fluorescence spectrophotometry in a 96-well plate format. A microtiter plate reader (SPECTRAmax GEMINIXS, Molecular Devices, Sunnyvale, CA) was set up as follows: excitation wavelength, 397 nm; emission wavelength, 466 nm; cut off wavelength, 420 nm; temperature, 30 °C. Under these conditions, there was no interference from the substrate 7-ethoxycoumarin. A series of eight solutions of 7-ethoxycoumarin (0–2 mM) were prepared by successive dilutions of a stock solution of 10 mM 7-ethoxycoumarin in Me_2SO into 50 mM potassium phosphate buffer, pH 7.8. The maximum final concentration of Me_2SO was 10% (v/v) Me_2SO. From this series, 185 μl was transferred into wells of the 96-well plate. 5 μl of P450 RhF from a 3.4 μM stock solution was added (0.086 μM) into each well and equilibrated for 3 min at room temperature. The reaction was initiated by addition of 10 μl of NAD(P)H solution from a freshly prepared stock (10 mM) using an 8-channel pipette. The plate was then immediately placed into the plate reader. The plate was shaken for 5 s to ensure thorough mixing, and then time-based measurements were recorded every 15 s for 10 min. The rate of formation of 7-hydroxycoumarin was calculated using an extinction-emission coefficient of $\epsilon = 1502\ mM^{-1}$, which was determined using 7-hydroxycoumarin standards.

For the inhibition studies, each inhibitor (either 5 or 10 mM) was pre-incubated with the assay mix (minus cofactor) for 5 min prior to initiating the reaction with NADPH. A negative control was also included in which no inhibitor was added. Steady state consumption of NADPH or NADH by P450 RhF could be measured using $K_3[Fe(CN)_6]$ as an artificial electron acceptor. In a typical reaction, 1 mM (a saturating concentration) of $K_3[Fe(CN)_6]$ in phosphate buffer was incubated with 5–6 nM of P450 RhF for 3 min and the reaction was initiated by addition of either NADH or NADPH at different concentrations (0–60 μM). The reaction was monitored at 340 nm (30 °C) for 10 min using a microtiter plate reader (VERSAmax, Molecular Devices).

Optically Transparent Thin Layer Electrochemical (OTTLE) Potentiometry—Spectroelectrochemical analysis of P450 RhF was conducted in an OTTLE cell constructed from a modified quartz EPR cell with a 0.3-mm path length, containing a Pt/Rh (95/5) gauze working electrode (wire diameter 0.06 mm, mesh size 1024 cm^{-1}), a platinum wire counter electrode and a Ag/AgCl reference electrode (model MF2052; Bioanalytical Systems, West Lafayette, IN). Enzyme samples (0.5 ml × 100–200 μM) were eluted through a G25 column pre-equilibrated with 0.1 M Tris-HCl, pH 7.5, 0.5 M KCl in an anaerobic glove box. The following mediators: pyocyanine (10 μM), 2-hydroxy-1,4-napthoquinone (20 μM), FMN (5 μM), benzyl viologen (10 μM), and methyl viologen (10 μM) were then added. Spectroelectrochemical titrations were performed at 25 ± 2 °C using an Autolab PGSTAT10 potentiostat and a Cary 50 UV/vis spectrophotometer. The potential of the working electrode was decreased in 30 mV steps until the enzyme was fully reduced and increased stepwise until reoxidation was complete. After each step the current and UV/vis absorption spectrum were monitored until no further change occurred. This equilibration process typically lasted 15 min. Absorbance changes at 418 nm (heme) and 462 nm (FMN) were plotted against the potential of the working electrode and analyzed simultaneously using the Nernst equation. The Ag/AgCl reference electrode employed in the OTTLE cell was calibrated against indigotrisulfonic acid ($E_m = -99$ mV *versus* SHE) and FMN ($E_m = -220$ mV *versus* SHE) in the same buffer conditions. All electrode potentials were corrected accordingly by +205 ± 2 mV relative to the standard hydrogen electrode.

RESULTS

Recombinant Expression—The expression construct (pAG04) was introduced into *E. coli* BL21(DE3), and the resultant cell extracts analyzed by SDS-PAGE. A band corresponding to the predicted molecular mass of the recombinant protein was visible on Coomassie-stained gels of the expression strain, which was absent from the control strain (*E. coli* BL21(DE3)pET14b). The identity of this band was confirmed by Western blot analysis using an anti-His tag antibody. Although we observed significant levels of recombinant protein from cell extracts of the expression strain grown in the absence of IPTG (*i.e.* leaky expression), protein purified from these preparations was generally subject to substantial proteolytic degradation. Subsequent analysis of whole cell extracts by Western blotting confirmed that much of this proteolysis was occurring in the cell prior to disruption (data not shown). In order to minimize this problem, all subsequent protein preparations were derived from cells grown in a fermentor to a low cell density (OD ~0.4), induced with IPTG, and then harvested shortly afterward (See "Experimental Procedures"). The level of recombinant P450 RhF peaked at about 3 h after induction (Fig. 1).

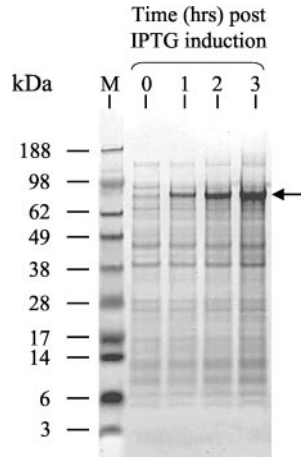

FIG. 1. **SDS-PAGE analysis of whole cell extracts of a culture of *E. coli* BL21(DE3)pAG04 following induction with IPTG.** The *arrow* indicates the position of the recombinant protein. Molecular mass markers are shown in *lane M*.

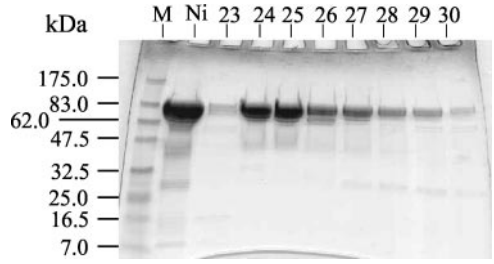

FIG. 2. **SDS-PAGE analysis of Resource Q column chromatography during purification of recombinant His_6-P450 RhF.** *Lane Ni*, pooled fractions from HiTrap Nickel column loaded onto Resource Q column; *lanes 23–30* show fractions from anion exchange chromatography on Resource Q column. Fractions 24–25 were used for analysis. Molecular mass markers are shown in *lane M*.

His_6-P450 RhF was purified using metal ion affinity and anion-exchange chromatography (Fig. 2). The His tag was then efficiently removed by treatment with thrombin. Removal of the tag was confirmed by both Western blot analysis using an anti-His tag antibody and by mass spectrometry (Fig. 3). We could detect no evidence of adventitious proteolysis at sites outside the targeted scissile bond.

Spectrophotometric Characterization—UV-visible absorption spectroscopy provides the basic technique for the recognition and characterization of cytochrome P450 enzymes. Recombinant His_6-P450 RhF and recombinant P450 RhF lacking the His tag gave essentially identical UV-visible absorption spectra that are typical of P450 hemoproteins (14). The oxidized form of purified P450 RhF displays the general spectral properties of

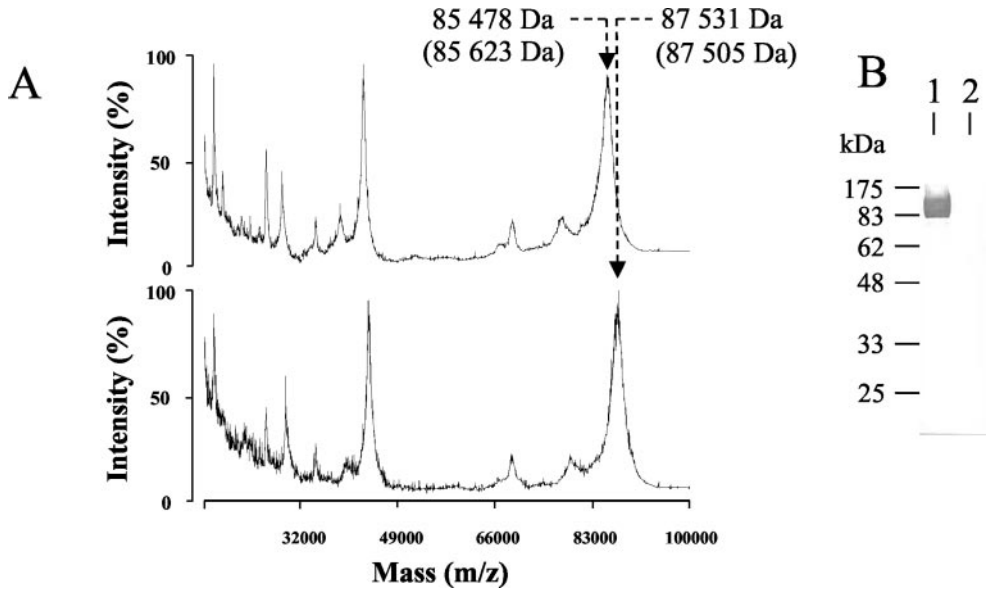

FIG. 3. **Analysis of thrombin-treated His_6-P450 RhF.** *Panel A*, MALDI-TOF analysis of protein before (*bottom*) and after (*top*) treatment with thrombin. The experimentally determined mass along with the predicted mass in parentheses (based on the sequence data) are highlighted by *arrows* for the singly charged species. *Panel B*, Western blot of His_6-P450 RhF before (*lane 1*) and after (*lane 2*) thrombin treatment using an anti-polyhistidine antibody. The same amount of protein (5 μg) was loaded in each lane. SDS-PAGE analysis of the samples showed no apparent differences before and after treatment with thrombin (data not shown).

cytochrome P450 enzymes with the major Soret band located at 424 nm, and the smaller α and β peaks at 574 and 539 nm, respectively (Fig. 4). Upon reduction with sodium dithionite, the Soret band shifts to 423 nm and diminishes in intensity. Subsequent bubbling of CO through the solution of dithionite-treated P450 RhF resulted in the characteristic shift of the Soret band to 450 nm. The CO-difference spectrum displays the prominent peak at 450 nm (Fig. 4, *inset*). The spectral characteristics of the enzyme remained unchanged after 3 months storage at −20 °C in 50% (v/v) glycerol. P450 RhF with and without the His tag display the same spectral properties, suggesting that the presence of these additional residues at the N terminus does not perturb the heme environment. Interestingly when the His tag was engineered onto the C terminus of P450 RhF the purified enzyme displayed the same spectral characteristics but was enzymatically inactive (data not shown). In this case the His tag may have perturbed the [2Fe-2S] cluster, thereby interfering with the electron transfer process.

Nucleotide Preference of P450 RhF—In order to determine the pyridine-nucleotide preference of P450 RhF, both pre-steady state and steady state experiments were performed. The direct reduction of the FMN group was monitored using stopped-flow spectrophotometry and the resulting plots of k_{obs} *versus* nucleotide concentration can be seen in Fig. 5. These gave rise to values for NADPH of $K_d = 6.6 \pm 0.8$ μM and $k_{lim} = 180 \pm 5$ s^{-1} with the corresponding values for NADH being $K_d = 3.7 \pm 0.3$ mM and k_{lim} 111 ± 5 s^{-1}. The P450 RhF catalyzed steady state oxidation of NAD(P)H using ferricyanide as an artificial electron acceptor also showed this cofactor preference. The NADPH-dependent reduction of potassium ferricyanide gave a k_{cat} of 39 ± 1 s^{-1} and a K_m of 6.6 ± 0.4 μM whereas NADH gave a k_{cat} of 16 ± 2 s^{-1} and a K_m of 0.18 ± 0.04 mM. These results make it clear that P450 RhF has a large preference for NADPH rather than NADH.

Kinetics of 7-Ethoxycoumarin Dealkylation—P450 RhF catalyzes the *O*-dealkylation of 7-ethoxycoumarin to form 7-hydroxycoumarin. The kinetic results obtained for His_6-P450 RhF were essentially the same as for the recombinant protein in which the His tag had been removed. The steady state kinetics

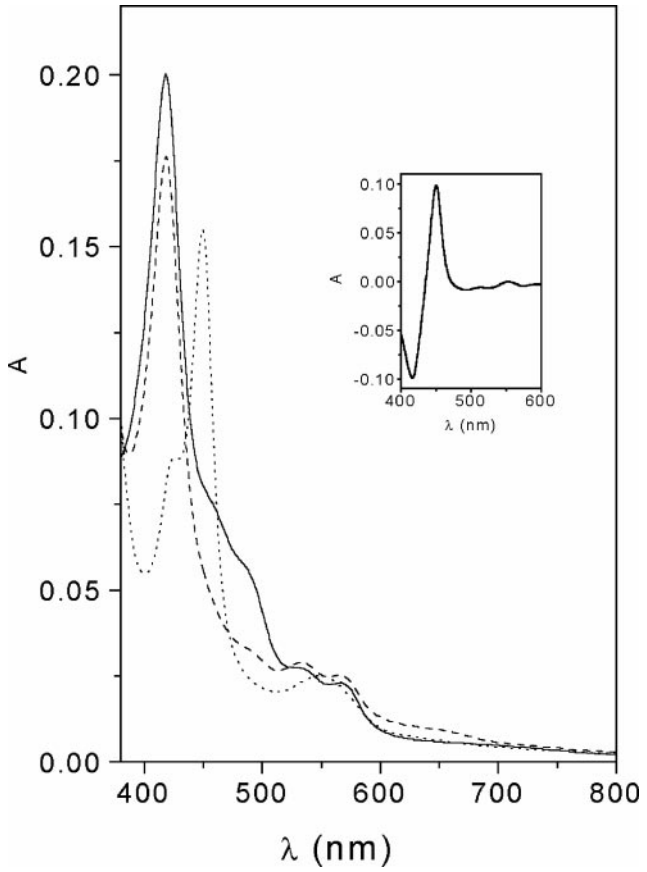

FIG. 4. **UV-visible absorption spectrum for purified P450 RhF (0.6 μM): oxidized (*solid line*), dithionite reduced (*dashed line*), and CO-bubbled (*dotted line*) are shown.** The difference spectrum generated by subtracting the spectrum for ferrous P450 RhF from the ferrous-carbon monoxy form is also shown (*inset*).

of the *O*-dealkylation of 7-ethoxycoumarin obeyed Michaelis-Menten kinetics and a typical plot of rate *versus* substrate concentration is shown in Fig. 6. Steady state parameters, k_{cat}

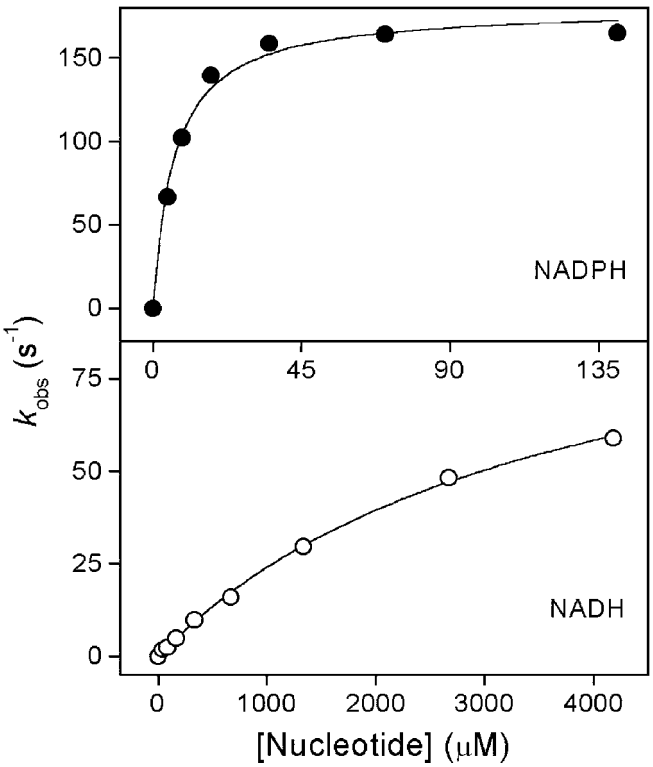

FIG. 5. **Saturation curves plotting k_{obs} *versus* nucleotide concentration for the pre-steady state (stopped-flow) reduction of the FMN in cytochrome P450 RhF by NADPH and NADH (at 25 °C and pH 7.5).** The data were fitted to a rectangular hyperbolic function to give values of K_d and k_{lim}. NADPH (●): $K_d = 6.6 \pm 0.8$ μM, $k_{lim} = 180 \pm 5$ s^{-1}. NADH (○): $K_d = 3.7 \pm 0.3$ mM, $k_{lim} = 111 \pm 5$ s^{-1}.

and K_m were 4.9 ± 0.1 min^{-1} and 0.22 ± 0.01 mM, respectively.

The fluorescent properties of 7-hydroxycoumarin, which differ from 7-ethoxycoumarin, allowed us to accurately and directly determine a low level of substrate turnover without the need for indirect measurement of NADPH consumption. The latter method is usually problematic due to both self-oxidation and the low level of coupling efficiency often associated with unnatural compounds acting as substrates. Nevertheless we also analyzed the rate of depletion of NADPH by monitoring the absorbance at 340 nm (data not shown). By comparing these results with those obtained from the direct measurement of product formation we estimate the coupling efficiency is between 10–15%.

P450 RhF activity against 7-ethoxycoumarin is inhibited by a number of general P450 inhibitors. The K_i values for three of these compounds were determined: 4-phenylimidazole, 0.8 ± 0.1 mM; 1-phenylimidazole, 1.6 ± 0.1 mM; and metyrapone, 2.5 ± 0.3 mM. All compounds inhibited the formation of product in a competitive fashion. This is illustrated graphically, in Fig. 7, for the inhibition by 1-phenylimidazole.

P450 RhF activity was unaffected by varying the concentration of salt (NaCl) up to 500 mM. Me_2SO was used as a solvent to dissolve the substrate. We found that the level of Me_2SO could be used up to 25% (v/v) in our reaction mix without adversely affecting the activity.

Potentiometry—The spectroelectrochemical analysis of P450 RhF was conducted using optically transparent thin layer electrochemical (OTTLE) potentiometry. The results from these experiments can be seen in Fig. 8. No hysteresis was observed in any of the potentiometric experiments indicating full equilibration and reversibility during the procedure. The Nernst curves shown in Fig. 8 show the large separation between the reduction potentials for the heme and flavin groups. This made the fitting of the data very straightforward, giving reliable and accurate values. The two-electron reduction potential for the FMN group was found to be −243 ± 15 mV (*versus* NHE). It was not possible to accurately determine the two one-electron potentials for the oxidized/semiquinone and semiquinone/reduced couples of the FMN although there was evidence for a small amount of semiquinone formation (seen as a long-wavelength, 600 nm, absorbance in Fig. 8) during the potentiometric experiment. The one-electron reduction potential of the heme group, in the absence of any substrate, was determined to be −423 ± 10 mV (*versus* NHE).

DISCUSSION

Previously we had reported the cloning of P450 RhF, an unusual cytochrome P450 in which the heme domain is fused to a phthalate-family oxygenase reductase (9). The cloning strategy involved a PCR-based screen for P450-like sequence elements and required no prior knowledge of the target enzyme substrate specificity. Hence nothing is known about the likely natural function of P450 RhF, although we are currently investigating its substrate specificity by screening against a library of compounds.[2] Nevertheless we reported that a recombinant strain of *E. coli* harboring the gene encoding P450 RhF is able to mediate the *O*-dealkylation of 7-ethoxycoumarin in whole cell biotransformation (9). However, the anticipated self-sufficiency of P450 RhF was not definitively demonstrated in these experiments since the possibility that endogenous *E. coli* redox proteins had supplied reducing equivalents to the recombinant protein *in vivo* could not be eliminated.

In the present study we have purified the recombinant His-tagged P450 RhF to apparent homogeneity. The catalysis of the *O*-dealkylation reaction followed Michaelis-Menten kinetics and the steady state parameters for the reaction were determined. Subsequent removal of the His tag by treatment with thrombin did not affect enzyme activity. We have therefore demonstrated the ability of the isolated enzyme to mediate catalysis in the absence of additional redox proteins. P450 RhF represents the first example of a self-sufficient cytochrome P450 that does not possess a primary structural organization akin to that of P450 BM3.

Three general inhibitors of P450 enzymes were found to inhibit the *O*-dealkylation reaction and the K_i value for each was determined. The three inhibitors are pyridine and imidazole derivatives that are thought to simultaneously bind to the lipophilic regions of the protein as well as the heme iron in a reversible manner (14). A double-reciprocal plot of enzyme kinetics in the presence and absence of inhibitor clearly demonstrated competitive inhibition, which confirms that the *O*-dealkylation reaction is indeed catalyzed by P450 RhF at the heme active site.

Direct measurement of the reduction of the FMN group by pyridine nucleotides showed that the enzyme displays a marked preference for NADPH over NADH. This degree of preference is almost entirely at the level of cofactor binding since there is only a very small difference (less than 2-fold) in the rate constant for FMN reduction whereas there is a very large (500-fold) difference in the dissociation constants. From sequence alignments and by analogy with the phthalate family of oxygenase reductase enzymes we had originally predicted that P450 RhF would be an NADH-dependent enzyme.

Although P450 RhF uses FMN, in all other P450s it is FAD that receives the reducing equivalents from the pyridine nucleotide. In the microsomal P450s and P450 BM3, FMN is used to shuttle electrons from the FAD to the heme. Potentiometric analysis of P450 RhF shows that the FMN has a two-electron

[2] A. Çelik, personal communication.

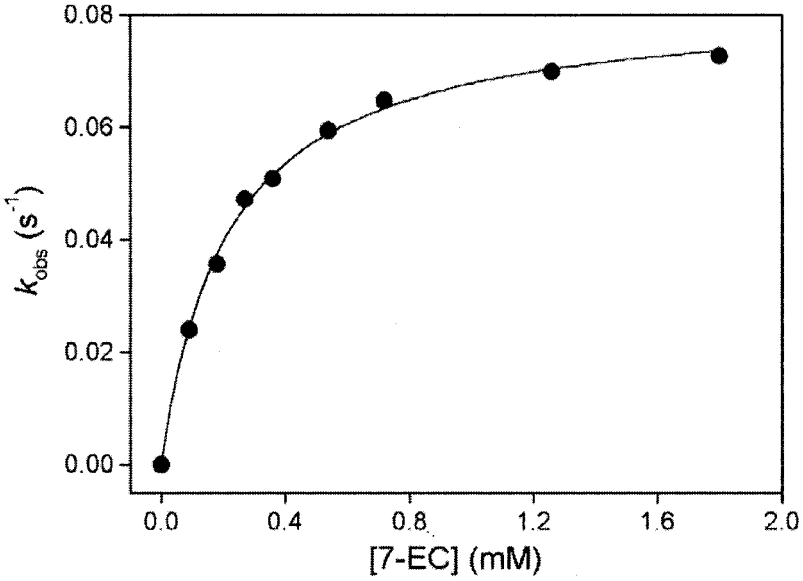

FIG. 6. **Michaelis-Menten curve for the NADPH-dependent *O*-dealkylation of 7-ethoxycoumarin catalyzed by P450 RhF.** NADPH was used as the electron donor.

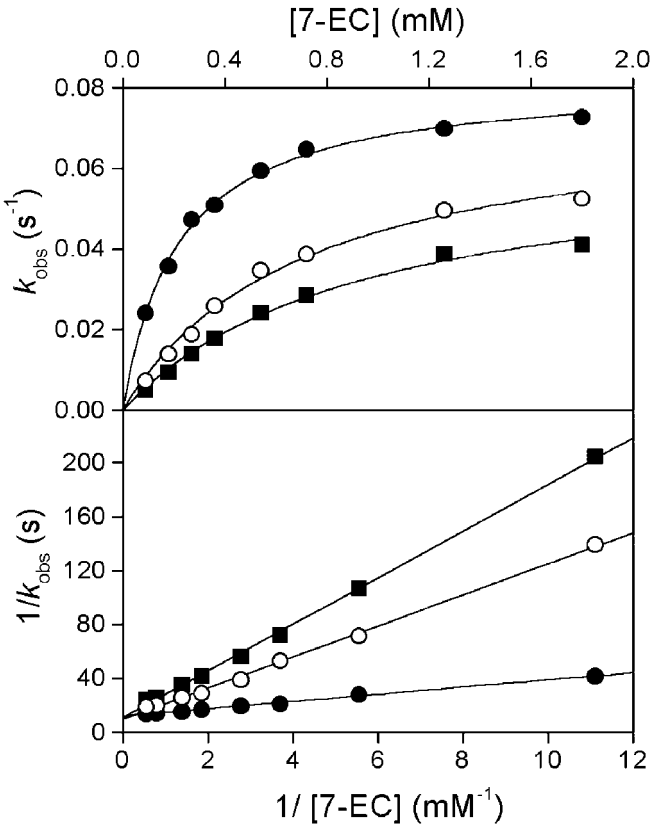

FIG. 7. **Inhibitor studies of P450 RhF.** Michaelis-Menten curves (*top*) and the corresponding Lineweaver-Burk plots (*bottom*) of the kinetics of *O*-dealkylation of 7-ethoxycoumarin in the absence (●-●) or presence of the inhibitor 1-phenylimidazole (○-○, 5 mM and ■-■, 10 mM).

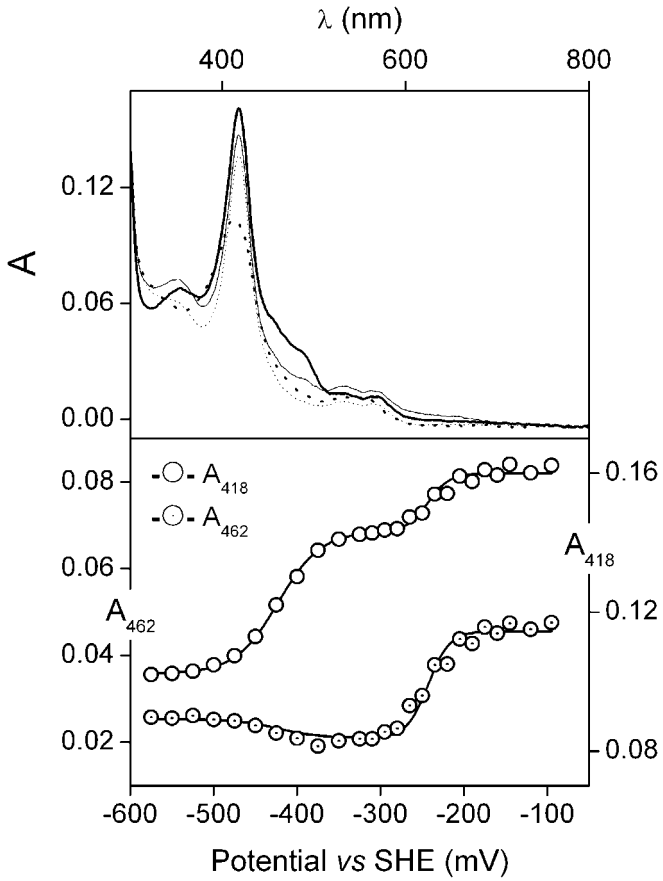

FIG. 8. **Potentiometric titration of intact P450 RhF.** The *upper panel* shows visible absorption spectra of the key intermediate redox states of the protein during the titration: $heme_{ox}$:FMN_{ox} (*thick solid line*), $heme_{ox}$:FMN_{sq} (*thin solid line*); $heme_{ox}$:FMN_{red} (*thin hatched line*); $heme_{red}$:FMN_{red} (*thick hatched line*). *Lower panel* shows the variation in absorbance with applied potential. *Open circles* correspond to absorption changes primarily associated with the heme ($A_{418\ nm}$, right axis), *open-dot circles* correspond to absorption changes primarily associated with the FMN ($A_{462\ nm}$, left axis). The data are fitted simultaneously to two-electron Nernst equations as described under "Experimental Procedures," using Microcal Origin 7.

reduction potential of −243 ± 15 mV. This is well poised for reduction by NADPH which has a reduction potential around −320 mV. A value of −243 mV is not untypical for flavin-containing reductases and lies between the two-electron reduction potentials of the FAD and FMN in P450 BM3 which are around −300 and −200 mV, respectively (15).

The reduction potential for the heme, in the absence of substrate, was found to be −423 ± 10 mV. This is identical, within experimental error, to the substrate-free heme potential seen for P450 BM3, reported as −427 ± 4 mV (16). In P450 BM3 (and many other P450s) it has been shown that the binding of substrate causes a change in the spin state of the heme-iron, from low to high spin. Accompanying this spin state change is

a large positive shift in reduction potential of around 130 mV (16). This change is spin-state and potential is required for efficient delivery of electrons from the reductase to the heme. Clearly a similar change would be required for efficient electron transfer to the heme in P450 RhF. Unfortunately, to date, binding trials with a variety of possible substrates have failed to produce any significant perturbation of the spin state. This lack of spin state change is probably the primary reason for the poor turnover rates and low coupling seen with a substrate such as 7-ethoxycoumarin.

Although the turnover of 7-ethoxycoumarin to 7-hydroxycoumarin is quite low (about 5 μmol of substrate turned over per 1 μmol of P450 RhF per minute), the primary objective of this study was to show self-sufficiency. Nevertheless, this single polypeptide electron transfer route could well support high catalytic activity. Indeed, the catalytic activity of P450 BM3 is the highest determined for a P450 monooxygenase (17,000 min^{-1} for arachidonate) (17). Such high activity is due in large part to the highly efficient electron transfer from the NADPH cofactor *via* the reductase to the P450 heme within a single polpeptide chain (18, 19). The correlation between efficient electron transfer housed on a single polypeptide and a high level of substrate turnover, as observed for P450 BM3, is probably a general feature of this type of P450 enzyme.

The identity of the likely natural substrate(s) for P450 RhF is currently unknown. Discovery of a natural substrate will also help elucidate the physiological role of P450 RhF and possibly its counterparts in other organisms. As pointed out by De Mot and Parret (8) these enzymes are present in phylogenetically unrelated bacteria. It will be intriguing to determine whether the function of the enzymes is conserved among these diverse organisms.

In the well-characterized phthalate dioxygenase, the intramolecular electrons flow from NADH to the semiquinone FMN and then to the [2Fe-2S] redox cluster (20). The significant degree of sequence homology between these reductases and the C-terminal portion of P450 RhF suggests that they possess*, mutatis mutandis*, a similar mechanism. We are currently dissecting the individual electron transfer steps by a combination of stopped-flow studies involving intact P450 RhF and mixed domain fragments. Fundamental studies into the electron transfer mechanism will provide valuable information concerning domain interactions for efficient electron transport and catalysis in these enzymes.

Acknowledgments—We thank Hannah Florance (Institute of Cell and Molecular Biology, University of Edinburgh) for assistance with the MALDI-TOF analysis and Simon Daff (School of Chemistry, University of Edinburgh) for useful discussions.

REFERENCES

1. Nerbert, D. W., and Gonzalez, F. J. (1987) *Annu. Rev. Biochem.* **56,** 945–993
2. Narhi, L. O., and Fulco, A. J. (1986) *J. Biol. Chem.* **261,** 7160–7169
3. Ravichandran, K. G., Boddupalli, S. S., Hasermann, C. A., Peterson, J. A., and Deisenhofer, J. (1993) *Science* **261,** 731–736
4. Kunst, F., Ogasawara, N., Moszer, I., Albertini, A. M., Alloni, G., Azevedo, V., Bertero, M. G., Bessieres, P., Bolotin, A., Borchert, S., Borriss, R., Boursier, L., Brans, A., Braun, M., Brignell, S. C., Bron, S., Brouillet, S., Bruschi, C. V., Caldwell, B., Capuano, V., Carter, N. M., Choi, S.-K., Codani, J.-J., Connerton, I. F., Cummings, N. J., Daniel, R. A., Denizot, F., Devine, K. M., Dusterhoft, A., Ehrlich, S. D., Emmerson, P. T., Entian, K. D., Errington, J., Fabret, C., Ferrari, E., Foulger, D., Fritz, C., Fujita, M., Fujita, Y., Fuma, S., Galizzi, A., Galleron, N., Ghim, S.-Y., Glaser, P., Goffeau, A., Golightly, E. J., Grandi, G., Guiseppi, G., Guy, B. J., Haga, K. *et al.* (1997) *Nature* **390,** 249–256
5. Yu, T.-W., Bai, L., Clade, D., Hoffmann, D., Toelzer, S., Trinh, K. Q., Xu, J., Moss, S. J., Leistner, E., and Floss, H. G. (2002) *Proc. Natl. Acad. Sci. U. S. A.* **99,** 7968–7973
6. Kitazume, T., Takaya, N., Nakayama, N., and Shoun, H. (2000) *J. Biol. Chem.* **275,** 39734–39740
7. Seo, J.-A., Proctor, R. H., and Plattner, R. D. (2001) *Fungal Genet. Biol.* **34,** 155–165
8. De Mot, R., and Parret, A. H. A. (2002) *Trends Microbiol.* **10,** 502–508
9. Roberts, G. A., Grogan, G., Greter, A., Flitsch, S. L., and Turner, N. J. (2002) *J. Bacteriol.* **184,** 3898–3908
10. Nagy, I., Schoofs, G., Compernolle, F., Proost, P., Vanderleyden, J., and De Mot, R. (1995) *J. Bacteriol.* **177,** 676–687
11. Sambrook, J., Fritsch, E. F., and Maniatis, T. (1989) *Molecular Cloning: A Laboratory Manual*, 2nd Ed., Cold Spring Harbor Laboratory, Cold Spring Harbor, NY
12. Grogan, G., Roberts, G. A., Bougioukou, D., Turner, N. J., and Flitsch, S. L. (2001) *J. Biol. Chem.* **276,** 12565–12572
13. Omura, T., and Sato, R. (1964) *J. Biol. Chem.* **239,** 2370–2378
14. Ortiz de Montellano, P. R. (1995) *Cytochrome P450, Structure, Mechanism, and Biochemistry*, 2nd Ed., pp. 305–364, Plenum Publishing Corp., New York
15. Daff, S. N., Chapman, S. K., Turner K. L., Holt, R. A., Govindaraj, S., Poulos, T. L., and Munro, A. W. (1997) *Biochemistry* **36,** 13816–13823
16. Ost, T. W. B., Miles, C. S., Munro, A. W., Murdoch, J., Reid, G. A., and Chapman, S. K. (2001) *Biochemistry* **40,** 13421–13429
17. Noble, M. A., Miles, C. S., Chapman, S. K., Lysek, D. A., MacKay, A. C., Reid, G. A., Hanzlik, R. P., and Munro, A. W. (1999) *Biochem. J.* **339,** 371–379
18. Munro, A. W., Leys, D. G., McLean, K. J., Marshall, K. R., Ost, T. W. B., Daff, S., Miles, C. S., Chapman, S. K., Lysek, D. A., Moser, C. C., Page, C. C., and Dutton, P. L. (2002) *Trends Biochem. Sci.* **27,** 250–257
19. Munro, A. W., Daff, S., Coggins, J. R., Lindsay, J. G., and Chapman, S. K. (1996) *Eur. J. Biochem.* **239,** 403–409
20. Correll, C. C., Batie, C. J., Ballou, D. P., and Ludwig, M. L. (1992) *Science* **258,** 1604–1610